Construction and Building Materials 389 (2023) 131765

Contents lists available at ScienceDirect

Construction and Building Materials

journal homepage: www.elsevier.com/locate/conbuildmat

Energy dissipation capacity of an optimized structural lightweight perlite concrete

Mohammad Bakhshi [a,*], Ali Dalalbashi [b], Hassan Soheili [c]

[a] Department of Civil Engineering, University of Minho, Guimaraes, Portugal
[b] Engineering Department, University of Trás-os-Montes and Alto Douro, Vila Real, Portugal
[c] Faculty of Civil and Environmental Engineering, Tarbiat Modares University, Tehran, Iran

ARTICLE INFO

Keywords:
Expanded perlite
Lightweight concrete
Energy dissipation capacity
Compressive strength

ABSTRACT

The Perlite Light-Weight Concrete (PLWC) provides various advantages compared to normal concrete, such as lower weight and high energy dissipation. However, PLWC has a lower compressive strength and modulus of elasticity than normal concrete; an appropriate mix design can be found for structural engineering. The present study investigates the effects of different components of the PLWC mixture on the target parameters of density, compressive strength, energy dissipation capacity, and energy dissipation rate. The optimal PLWC mixture is identified based on the quality function defined by the target parameters. For this purpose, the Taguchi method is utilized to find the optimal mixture containing ten components in four levels, where the natural aggregate is partially replaced by the expanded Perlite. The effect of each mixture on the compressive strength and energy dissipation capacity of concrete is investigated. The results demonstrate that, however, existing of the expanded Perlite has a negative effect on the compressive strength, it improves the potential of concrete to dissipate energy. Also, expanded Perlite increases the energy dissipation rate of concrete and controls crack propagation. Optimized mixture with bulk density and compressive strength values of 1761 kg/m^3 and 21.3 MPa, respectively, shows the higher energy dissipation capacity of 0.1118 J. Finally, new models are proposed to express the compressive behavior of Perlite and its capacity to dissipate energy. The proposed models can significantly predict the energy dissipation capacity and energy dissipation rate of PLWC. Thus, the use of Perlite as a sustainable option is recommended for the production of lightweight and energy-efficient concrete structures.

1. Introduction

Lightweight concretes have received extensive attention using in construction due to decreasing the structure weight [1]. Compared to conventional concrete, lightweight concrete has a lower bulk density and better thermal insulation, is more cost-effective, and absorbs more energy [2–4]. A lightweight concrete mixture replaces the normal aggregates with lightweight coarse and fine aggregates, such as Leca, Perlite, and polystyrene [5–9]. The low porous structure and fire resistance of expanded Perlite make it the most popular of these materials [10].

Many studies [1,11–13] have examined the impact of Perlite on the thermal conductivity and durability of Perlite lightweight concrete (PLWC). In addition, the mechanical properties of PLWC were investigated as non-structural concrete. Expanded Perlite aggregate causes the density and heat transfer coefficient of lightweight concrete to improve over conventional concrete, while its compressive strength and modulus of elasticity decrease [1,11–18]. The reduction effect of adding expanded Perlite may be various in different concrete because of the effect of other components, such as Silica fume, fly ash, Sodium silicate (water glass), and superplasticizer [5]. Adding Silica fume increases the compressive strength and density of the PLWC [12,13,19] while using the superplasticizer leads to a decrease the strength [19]. PLWC can dissipate energy significantly, due to the fracture of expanded Perlite aggregates under impact loadings [5]. The studies illustrated that PLWC must have a satisfactory slump to prevent the fracture of Perlite during mixing [5]. In addition, PLWCs must be sufficiently sticky aggregates to overcome the floating force of Perlite owing to its low density [11]. Therefore, it is unknown what the mechanical behavior (including compressive strength, elastic modulus, and energy dissipation) of PLWC is as a structural concrete. Furthermore, research on performing optimized PLWC as a lightweight structural concrete under compressive

* Corresponding author.
E-mail address: Mohammad.bakhshi.ngd@gmail.com (M. Bakhshi).

https://doi.org/10.1016/j.conbuildmat.2023.131765
Received 26 January 2023; Received in revised form 1 May 2023; Accepted 10 May 2023
Available online 16 May 2023
0950-0618/

loading needs to be conducted in more depth.

The stress–strain behavior of concrete determines its energy absorption capacity, which is influenced by various factors, including the type and amount of cementitious materials, water-cement ratio, degree of compaction, aggregate type and size, curing conditions, and type of loading. The energy absorption capacity of concrete can be improved by using supplementary cementitious materials, such as fly ash or slag, and high-performance admixtures. These materials can modify the microstructure of concrete and enhance its toughness [20,21]. Additionally, incorporating fibers, such as steel or polypropylene, can reinforce the concrete and prevent sudden failure under compressive loading, thus increasing its energy absorption capacity [22,23].

This study aims to investigate the compressive behavior of the structural PLWCs with different components in more depth. The key parameters to explain compressive behavior are compressive strength, modulus of elasticity, peak strain, and energy dissipation capacity. The effect of different components on the mechanical and physical behavior of PLWCs is investigated, and the optimized proportions of PLWC's component parts are determined in order to be used in structural concrete. These proportions include the amount of expanded Perlite aggregates, cement content, pozzolans (Silica fume and Slag), water-to-cement ratio (w/c), filler (Glass and Quartz powders), Sodium silicate, and superplasticizer. For this purpose, new models are proposed to express the compressive strength, modulus of elasticity, and energy dissipation capacity of the PLWCs under compressive loading. In addition, an experimental program has been performed to find the best mix design for PLWC using a practical quality function based on the energy dissipation capacity of specimens under compressive loading, material properties, and the bulk density of concrete. Ultimately, this study proposes novel models for characterizing the compressive behavior and energy dissipation capacity of Perlite. The findings support the advancement of sustainable and energy-efficient construction materials while offering a viable solution to producing structural lightweight concrete.

2. Experimental program

2.1. Materials

Table 1 presents the materials used and their chemical properties. Hydraulic cement Portland type II was used with a specific density of 3.15 gr/cm^3 and the normal consistency of 27.6% determined based on ASTM C150 [24] and ASTM C187 [25], respectively. The mix also includes Sodium silicate (or water glass) to improve its porous structure [26], with a density of 2.41 gr/cm^3.

In this study, both normal and lightweight coarse aggregates were used. The density and maximum size of the normal aggregate were 2.59 gr/cm^3 and 19 mm. As a lightweight aggregate, expanded Perlite was used (Fig. 1) with a density of 0.25 gr/cm^3. When the raw Perlite was exposed to high thermal shock, its Silica microstructures were softened due to heat and lose their internal water rapidly. The process caused various holes to form in the Perlite aggregates, resulting in its expansion of 10–20 times.

Glass and quartz powder fillers were used to improve particle packing and concrete performance, as well as reduce cement content without sacrificing strength [27]. The density and the maximum size of glass powder were 2.56 gr/cm^3 and 75 μm. These values for the quartz powder were 2.79 gr/cm^3 and 200 μm, respectively.

The mix also included Silica fume to improve its porous structure [26], strength, and durability [28,29]. The Silica fume contained 94 ~ 96% SiO_2 and its density equaled 2.10 gr/cm^3, about three times its bulk density. The ground granulated blast-furnace Slag (GGBS) was applied as another mineral supplement ingredient to replace cement and minimize its costs. Using Slag also increases the workability and strength of concrete [30]. The Slag had a density of 2.80 gr/cm^3 and fineness of 3500 cm^2/gr with a particle size range of 1 to 10 μm. Since expanded Perlite aggregates were utilized to decrease the concrete density to a lightweight range, slag, silica fume, and glass powder were incorporated to maintain the compressive strength and mechanical properties within the range of structural concrete.

Type Flowcem R500 superplasticizer based on polycarboxylate was added to all mixtures to increase concrete flow while reducing water usage and avoiding aggregate separation. The superplasticizer was a light-yellow-colored liquid that had a minimum pH of 5. Also, at an ambient temperature of 20 °C, the volumetric mass of the superplasticizer was 1.09 gr/cm^3.

2.2. Mix design

In the present study, the Taguchi method [31] was used to determine the optimal mixtures of PLWC by considering the four characteristics of density, compressive strength, energy dissipation capacity, and energy dissipating rate. Taguchi Method is a process/product optimization method based on 8-steps of planning and evaluating results to determine the best levels of control factors [31]. The primary goal was to keep the variance in the output very low, even in the presence of noise inputs. Totally, ten variables were considered in Table 2 and four levels were defined for nine variables and two levels were defined for one variable, as listed in Table 2, [11,12,32–35]. Although increasing the number of specified levels improves the accuracy of the experimental investigation, it also increases the number of required samples, as well as the cost and time of casting and testing specimens. In the limited number of tests, the Taguchi method guides how the ten variables in 4 levels should be mixed to represent all sampling and determine the effective parameters.

In Taguchi statistical method, different special designs named as "orthogonal arrays" are used to study entire parameter space [31]. In the

Table 1
Chemical composition of the materials.

Material	SiO_2 [%]	Al_2O_3 [%]	Fe_2O_3 [%]	MnO [%]	MgO [%]	CaO [%]	Na_2O [%]	K_2O [%]	P_2O_5 [%]	TiO_2 [%]	Cl [%]	C [%]	S [%]	Sic [%]	Fe [%]	SO_3 [%]	H_2O [%]
Cement	21.70	4.62	3.95	–	1.25	65.04	0.62	0.61	–	–	–	–	–	–	–	2.78	–
Sodium silicate	28.83	–	–	–	–	–	9.29	–	–	–	–	–	–	–	–	–	61.88
Lightweight aggregate																	
Perlite	72.10	12.95	0.88	–	0.25	1.47	3.16	3.92	–	–	–	–	–	–	–	–	3.88
Filler																	
Glass powder	71.09	3.52	1.77	–	1.56	10.59	10.46	0.89	–	–	–	–	–	–	–	0.03	–
Quartz powder	99.50	0.13	0.01	–	–	0.02	–	0.001	–	0.002	–	–	–	–	–	0.04	–
Pozzolan																	
Silica fume	94–96	1.32	0.87	–	0.97	0.49	0.31	1.01	0.16	–	0.78	0.30	–	0.50	–	0.10	0.80
Slag	10.39	1.00	17.25	7.20	7.22	48.74	0.34	0.32	2.08	1.06	–	–	0.05	–	2.24	2.15	–

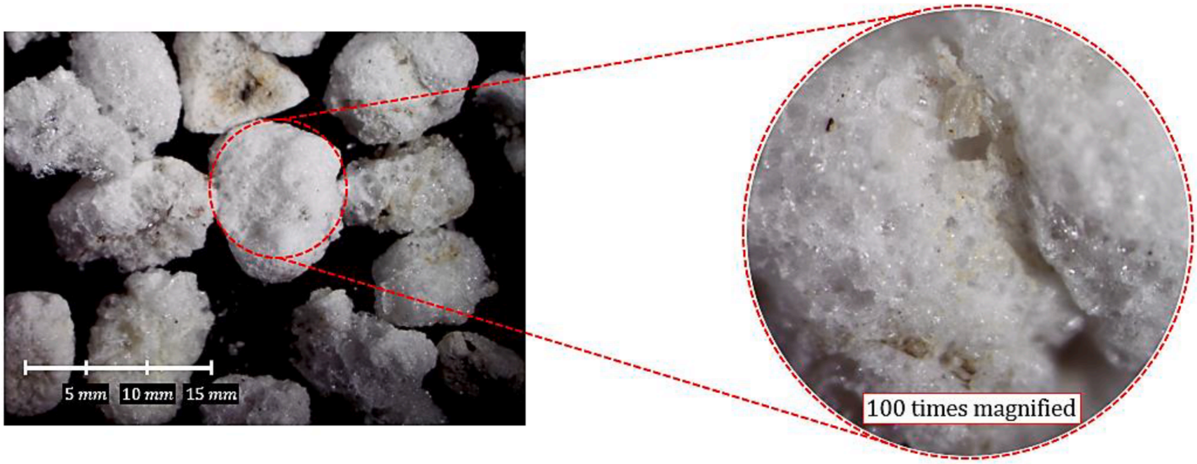

Fig. 1. Perlite aggregate.

Table 2
Levels of variables based on Taguchi method.

Variables	Level 1	Level 2	Level 3	Level 4
Cement amount [Kg/m^3]	400	450	500	550
Water/cement content (w/c)	0.38	0.41	0.44	0.47
Superplasticizer (SP) [%wt.]	0.0	0.2	0.4	0.6
Maximum size of normal aggregates [mm] *	12.5	19.0	–	–
Perlite replacement [%]	55	70	85	100
Sodium silicate (Water glass - WG) [% wt.]	1.75	2.50	3.25	4.00
Silica fume [%vol.]	8	10	12	14
Slag [%vol.]	10	18	26	32
Quartz powder [%wt.]	0	10	20	30
Glass powder [%wt.]	0	10	20	30

* Regarding the L-32 array in the Taguchi method, this variable is defined at two levels.

present study, the Taguchi L32 array was applied to determine the optimum conditions. Therefore, 32 experiments with specific mix designs were defined to enable the evaluation of PLWC characteristics, as listed in Table 3. Table 3 shows the value and level of each component for each mix design. For each mix proportion, three cylindrical specimens were cast (a total of 96 samples). A signal-to-noise ratio (S/N) for each output function is required to evaluate the discrepancy between the desired and experimental values [36]. In the Taguchi method, there are three distinct types of S/N ratios, namely lower is better (LB), nominal is better (NB), and larger or higher is better (HB) [5]. For the purpose of this study, the HB approach was selected since the objective was to determine the higher mechanical characteristics of the process under investigation.

2.3. Specimen preparation

A saturated surface dry (SSD) condition was considered for all aggregates, based on AASHTO T85 [37]. For this purpose, the saturated aggregates were stored at room temperature until the SSD conditions were reached. Afterward, the SSD-treated and dried aggregates were weighed to calculate their water content and modify the amount of water required for the mixtures. Preparation of specimens was performed by similar mixing steps, as follows: (1) First, aggregates were poured into the mixer; (2) The required amount of water was added to the mixer and mixed for one minute to achieve SSD mode.; (3) A slurry of cement and pozzolan was prepared with 80% water and mixed for two minutes.; (4) The superplasticizer and the remained water (20%) were combined and added to the mixer; and (5) After two minutes of mixing, the process was completed. Then specimens were cast and immersed in lime-saturated water at 23 °C for 28 days. Because of the interfacial transition zone (ITZ) bonding that determines PLWC strength [38], 28 days of curing were essential for achieving maximum strength. On the day of testing, specimens were capped to prepare for the compressive and elastic modulus test, based on ASTM C617 [39].

2.4. Materials characterization tests

Fresh concrete mixtures were prepared for the slump test to assess their flow properties, according to ASTM C143 [40]. The workability of all PLWCs was tested before molding the cylindrical specimens. In addition, the bulk density of mixes was determined based on ASTM C138 [41]. For each mix proportion, the bulk density test was performed three times.

Cylindrical specimens (with 150 mm diameter and 300 mm height) were prepared to determine the compressive strength and the modulus of elasticity of specimens, according to ASTM C39 [42] and ASTM C469 [43]. A Santam STM-2000 servo-electromechanical universal testing machine with a maximum loading capacity of 200 tons applied compressive load and three LVDTs with a 10 mm range and 100-μm sensitivity measured the deformation of the specimen. A load of 4.3 kN/sec was applied during the compressive strength test. Teflon sheets were used between the loading plates and concrete cylinders to remove the effect of friction and prevent multiaxial loading (Fig. 2).

3. Results and discussion

3.1. Physical properties

Fig. 3 shows the slump values of the mixtures from 3 mm to 288 mm. A lower value of slump in some mixtures is due to their high adhesion [35]. This phenomenon is significantly observed in mixtures with a lower amount of water, such as S1, S5, S25, and S29, as well as S6 and S23 with relatively high amounts of water and without superplasticizer. While some other mixtures (such as S4, S8, S11, S15, S16, S17, S21, and S26) had high slump values which are because of their higher water-to-cement ratios and to exist of water inside the Perlite aggregate. It means that, unlike normal aggregates, the water required for SSD condition of perlite aggregates can be removed from the Perlite during mixing, which leads to an increase in the slump of the mixture [11,44]. A high amount of superplasticizer (e.g., S3, S7, S9, S10) causes the slump value to rise. When different components are used, however, the slump value can be investigated more comprehensively. For instance, mixture S25 including 85% replaced Perlite demonstrates a low slump value, due to using the lowest water-to-cement ratio and superplasticizer. Therefore, water to

Table 3
Selected mix proportions based on the L-32 array in the Taguchi method.

Mix. No.	Cement [kg/m^3]	w/c	Superplasticizer [%wc [a]]	Max. Agg. Size [mm]	Perlite [%va [b]]	Water glass [%wc [a]]	Silica fume [%wc [a]]	Slag [%wc [a]]	Quartz powder [%wc [a]]	Glass powder [%wc [a]]
S1	400 (1)	0.38 (1)	0.0 (1)	12.5 (1)	55 (1)	1.75 (1)	8 (1)	10 (1)	0 (1)	0 (1)
S2	400 (1)	0.41 (2)	0.2 (2)	12.5 (1)	70 (2)	2.50 (2)	10 (2)	18 (2)	10 (2)	10 (2)
S3	400 (1)	0.44 (3)	0.4 (3)	12.5 (1)	85 (3)	3.25 (3)	12 (3)	26 (3)	20 (3)	20 (3)
S4	400 (1)	0.47 (4)	0.6 (4)	12.5 (1)	100 (4)	4.00 (4)	14 (4)	34 (4)	30 (4)	30 (4)
S5	450 (2)	0.38 (1)	0.2 (2)	12.5 (1)	55 (1)	4.00 (4)	10 (2)	34 (4)	20 (3)	20 (3)
S6	450 (2)	0.41 (2)	0.0 (1)	12.5 (1)	70 (2)	3.25 (3)	8 (1)	26 (3)	30 (4)	30 (4)
S7	450 (2)	0.44 (3)	0.6 (4)	12.5 (1)	85 (3)	2.50 (2)	14 (4)	18 (2)	0 (1)	0 (1)
S8	450 (2)	0.47 (4)	0.4 (3)	12.5 (1)	100 (4)	1.75 (1)	12 (3)	10 (1)	10 (2)	10 (2)
S9	500 (3)	0.38 (1)	0.6 (4)	12.5 (1)	70 (2)	4.00 (4)	12 (3)	26 (3)	0 (1)	10 (2)
S10	500 (3)	0.41 (2)	0.4 (3)	12.5 (1)	55 (1)	3.25 (3)	14 (4)	34 (4)	10 (2)	0 (1)
S11	500 (3)	0.44 (3)	0.2 (2)	12.5 (1)	100 (4)	2.50 (2)	8 (1)	10 (1)	20 (3)	30 (4)
S12	500 (3)	0.47 (4)	0.0 (1)	12.5 (1)	85 (3)	1.75 (1)	10 (2)	18 (2)	30 (4)	20 (3)
S13	550 (4)	0.38 (1)	0.4 (3)	12.5 (1)	70 (2)	1.75 (1)	14 (4)	18 (2)	20 (3)	30 (4)
S14	550 (4)	0.41 (2)	0.6 (4)	12.5 (1)	55 (1)	2.50 (2)	12 (3)	10 (1)	30 (4)	20 (3)
S15	550 (4)	0.44 (3)	0.0 (1)	12.5 (1)	100 (4)	3.25 (3)	10 (2)	34 (4)	0 (1)	10 (2)
S16	550 (4)	0.47 (4)	0.2 (2)	12.5 (1)	85 (3)	4.00 (4)	8 (1)	26 (3)	10 (2)	0 (1)
S17	400 (1)	0.38 (1)	0.6 (4)	19.0 (2)	100 (4)	3.25 (3)	8 (1)	18 (2)	10 (2)	20 (3)
S18	400 (1)	0.41 (2)	0.4 (3)	19.0 (2)	85 (3)	4.00 (4)	10 (2)	10 (1)	0 (1)	30 (4)
S19	400 (1)	0.44 (3)	0.2 (2)	19.0 (2)	70 (2)	1.75 (1)	12 (3)	34 (4)	30 (4)	0 (1)
S20	400 (1)	0.47 (4)	0.0 (1)	19.0 (2)	55 (1)	2.50 (2)	14 (4)	26 (3)	20 (3)	10 (2)
S21	450 (2)	0.38 (1)	0.4 (3)	19.0 (2)	100 (4)	2.50 (2)	10 (2)	26 (3)	30 (4)	0 (1)
S22	450 (2)	0.41 (2)	0.6 (4)	19.0 (2)	85 (3)	1.75 (1)	8 (1)	34 (4)	20 (3)	10 (2)
S23	450 (2)	0.44 (3)	0.0 (1)	19.0 (2)	70 (2)	4.00 (4)	14 (4)	10 (1)	10 (2)	20 (3)
S24	450 (2)	0.47 (4)	0.2 (2)	19.0 (2)	55 (1)	3.25 (3)	12 (3)	18 (2)	0 (1)	30 (4)
S25	500 (3)	0.38 (1)	0.0 (1)	19.0 (2)	85 (3)	2.50 (2)	12 (3)	34 (4)	10 (2)	30 (4)
S26	500 (3)	0.41 (2)	0.2 (2)	19.0 (2)	100 (4)	1.75 (1)	14 (4)	26 (3)	0 (1)	20 (3)
S27	500 (3)	0.44 (3)	0.4 (3)	19.0 (2)	55 (1)	4.00 (4)	8 (1)	18 (2)	30 (4)	10 (2)
S28	500 (3)	0.47 (4)	0.6 (4)	19.0 (2)	70 (2)	3.25 (3)	10 (2)	10 (1)	20 (3)	0 (1)
S29	550 (4)	0.38 (1)	0.2 (2)	19.0 (2)	85 (3)	3.25 (3)	14 (4)	10 (1)	30 (4)	10 (2)
S30	550 (4)	0.41 (2)	0.0 (1)	19.0 (2)	100 (4)	4.00 (4)	12 (3)	18 (2)	20 (3)	0 (1)
S31	550 (4)	0.44 (3)	0.6 (4)	19.0 (2)	55 (1)	1.75 (1)	10 (2)	26 (3)	10 (2)	30 (4)
S32	550 (4)	0.47 (4)	0.4 (3)	19.0 (2)	70 (2)	2.50 (2)	8 (1)	34 (4)	0 (1)	20 (3)

The number in parentheses indicates the level of each component in the mixtures.
[a] %va means volume percentage of aggregate.
[b] %wc means the weight percentage of cement.

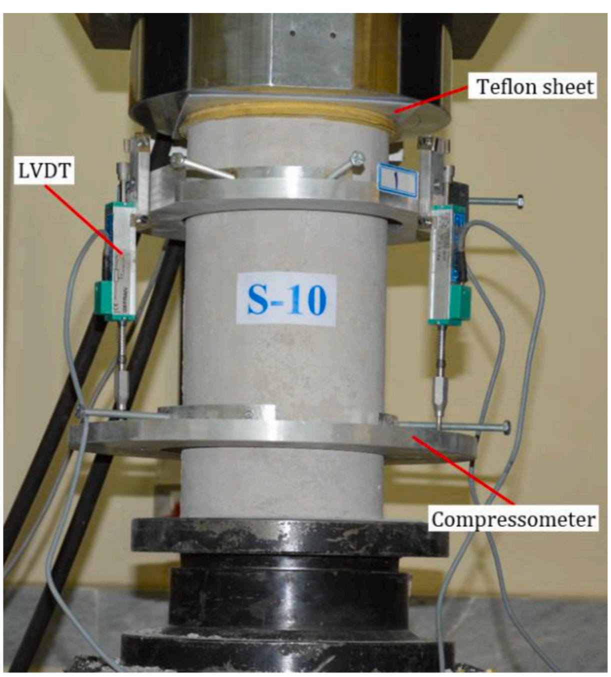

Fig. 2. Uniaxial compressive test.

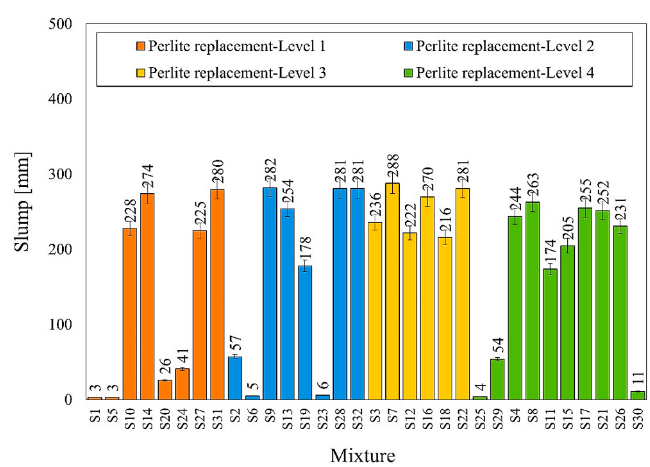

Fig. 3. The slump of the mixtures, with its standard deviation.

cement ratio, superplasticizer, and matrix adhesion due to water glass and pozzolan are effective parameters of the slump value.

Fig. 4 shows the density of mixes ranging from 1507 to 2068 kg/m^3 with a Coefficient of Variation (CoV) between 0.3% and 1.4%. Clearly, by increasing the amount of Perlite in PLWC, the density decreases due to the porous nature of the material. Moreover, a decrease in slump is associated with an increase in density. This observation contrasts with those in other studies [45–47] that used different lightweight aggregates (such as EPS, Leca, and pumice).

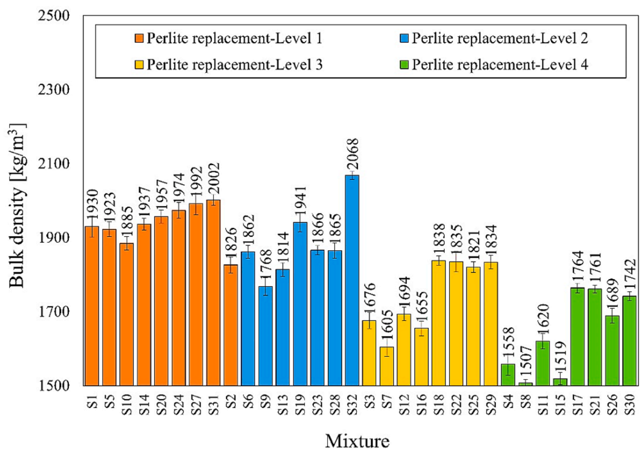

Fig. 4. Bulk density of mixtures, with its standard deviation.

3.2. Mechanical properties

Fig. 5 presents the compressive failure of specimens. Failure occurs with barreling in specimens with lower levels of Perlite aggregate (levels 1 and 2). While for specimens with a higher amount of Perlite aggregates (level 4), damage occurs more at the top than at the middle or bottom. As the expanded Perlite increases in volume, there may be local damage occurring and lateral strain reduced due to its low skeletal strength. In future studies, this observation needs to be explored in more detail.

Fig. 6 shows the fracture pattern of normal concrete and PLWC. Observation of the fracture pattern of PLWC reveals that crack propagation occurs through the aggregates, not in the Interfacial Transition Zone (ITZ). However, cracks did not always propagate into the stronger lightweight aggregate, especially in concrete with lower matrix strength. So, a balance between the matrix strength and aggregate strength should be available if the crack wants to spread into the aggregate. In this situation, the fracture surface exhibits broken and intact particles at the same time, and even some holes are caused by the premature detachment of the lightweight aggregate.

Fig. 7 and Table 4 present the average results of the specimens under compressive load, with a CoV between 2% and 9%. The results show that the maximum compressive strength is 34.8 MPa. The compressive strength is directly proportional to the aggregate crushing strength and density. The replacement of expanded Perlite due to its porous structure and low strength reduces the compressive strength of concrete which is in line with previous studies [1,5]. Moreover, the maximum modulus of elasticity is 15497 MPa. The effect of each component on the modulus of elasticity (initial tangent modulus) was like the compressive strength of PLWCs. However, the modulus of elasticity depends on various factors, such as water-to-cement ratio, components features and dispersion in the mixture, Perlite aggregates, and the characteristics of the transition zone [11].

3.3. Analyzing results by the Taguchi method

The results were analyzed by the Taguchi method in the Minitab software. This method determines the best machining parameters by measuring the signal-to-noise ratio (S/N) for each output function [36]. The highest S/N value (maximum absolute value) of the considered machining parameter levels indicates an optimal level. The effect of the 10 variables (as reported in Table 2) on the density, compressive strength, energy dissipation capacity, and energy dissipation rate are shown in Fig. 8 toFigure *11*, respectively. In these figures, the horizontal and vertical axis indicate each component's levels and their S/N values, respectively. Also, the dashed line shows the constant coefficient in the linear model analysis by the Taguchi method. The energy dissipation capacity is defined as the area under the stress–strain curve until the failure strain (ε_u). ε_u is the lowest value between 0.01 and the strain corresponding to $0.5f_{co}$ [32]. The energy dissipation rate ($\dot{\rho}_E$) of PLWC

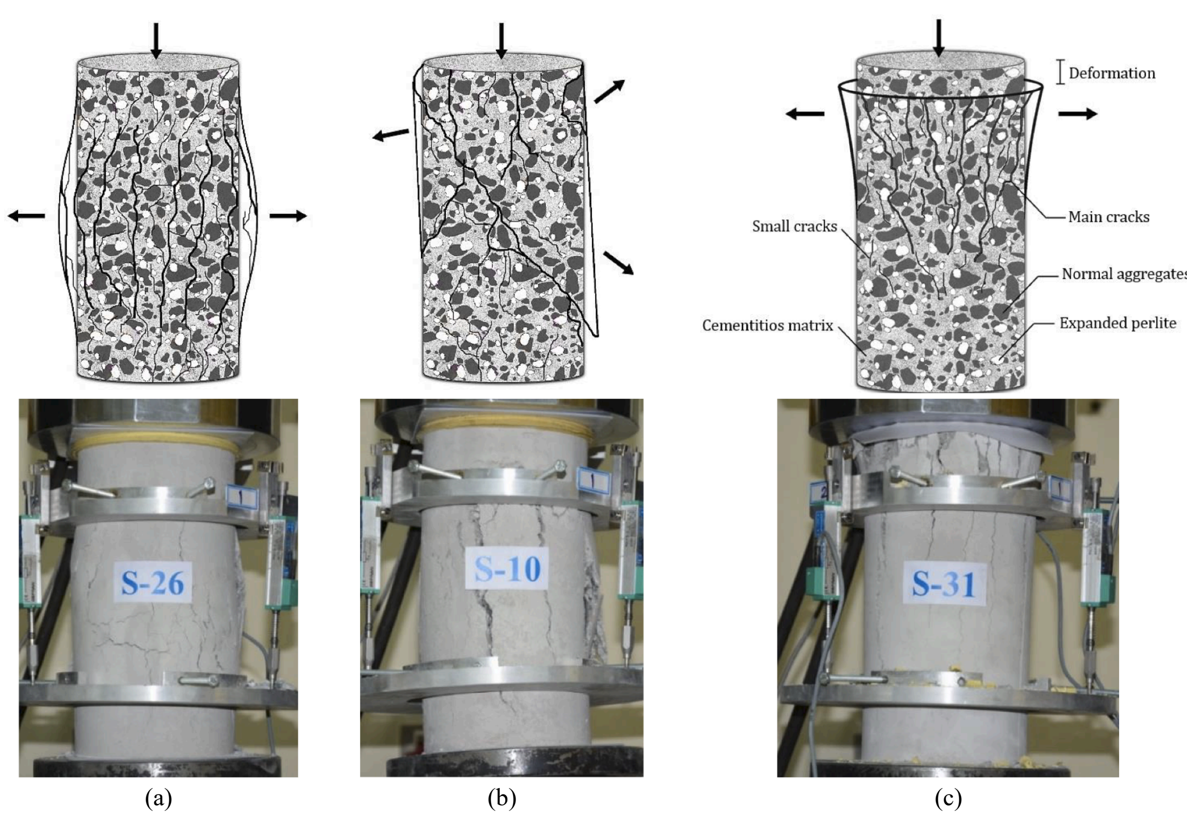

Fig. 5. Failure pattern for different expanded Perlite volumes (or levels): (a) Level 1; (b) Level 3; (c) Level 4.

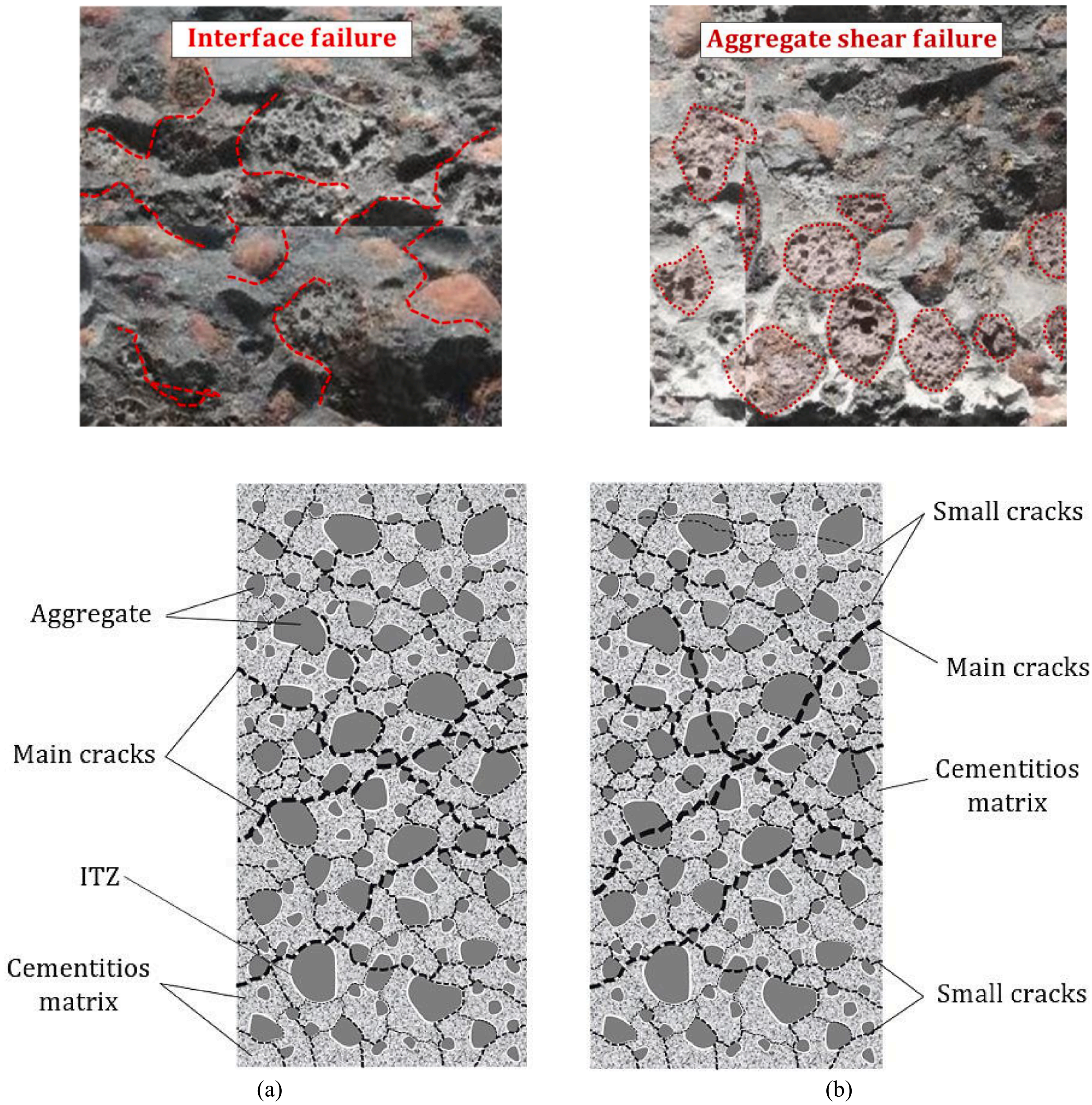

Fig. 6. Illustration of the fractured section of (a) normal concrete [5]; and (b) PLWC.

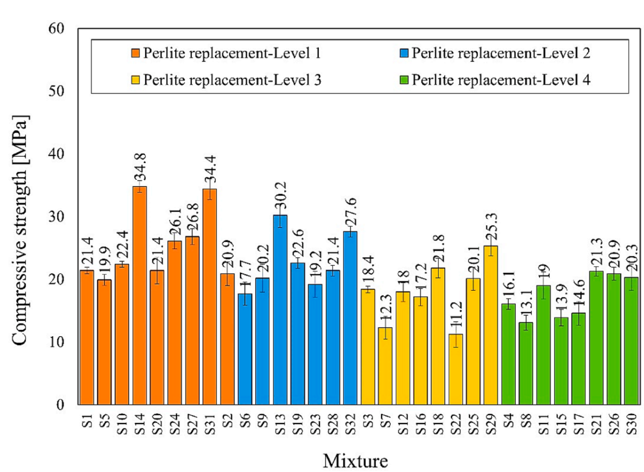

Fig. 7. Compressive strength of the mixtures, with its standard deviation.

specimens is also defined as the derivative of the energy dissipation capacity per unit volume overstrained.

3.3.1. *Density*

Water glass and cement content do not show a significant effect on the density, as presented in Fig. 8. In addition, increasing the water-to-cement ratio (w/c) over 0.41 (level 2) leads to a decrease in the density of the specimens. Density is determined by the number and size of pores in the specimens as a result of the hydration process of cement. Hence, the amount of water has a greater impact on hydration than the amount of cement.

The results illustrate that, by increasing the aggregate size, the density decreases. It can be because of the amount of porosity. By increasing the aggregate size, the ITZ zone surfaces decrease [48]. Since porosity forms in the ITZ zone more than matrix, the porosity decreases, and consequently the density increases [48]. However, adding Perlite as a porous lightweight aggregate appreciably decreases the density (see Fig. 8). More research should be conducted to better understand the influence of porosity on PLWC density.

Increasing the Silica fume (Micro silica) values causes density to

Table 4
Summary of obtained results.

Mix No.	Density [kg/m^3]	Slump [mm]	Compressive strength [MPa]	Modulus of elasticity [MPa]	Peak strain *	E_e [N.m]	$\dot{\rho}_E$ [N.m]
S1	1930	3	21.4	9851	2.77E-03	0.0925	8.17
S2	1826	57	20.9	11,303	2.52E-03	0.0646	4.70
S3	1676	236	18.4	10,205	2.50E-03	0.0695	5.77
S4	1558	244	16.1	9003	2.26E-03	0.0582	5.01
S5	1923	3	19.9	10,914	2.30E-03	0.0679	4.82
S6	1862	5	17.7	9941	2.36E-03	0.0676	5.06
S7	1605	288	12.3	8234	1.87E-03	0.0739	7.72
S8	1507	263	13.1	8981	2.06E-03	0.0731	7.09
S9	1768	282	20.2	11,166	2.52E-03	0.0860	7.18
S10	1885	228	22.4	11,574	2.66E-03	0.0812	5.87
S11	1620	174	19.0	11,099	2.35E-03	0.0669	5.24
S12	1694	222	18.0	10,458	2.35E-03	0.0601	4.41
S13	1814	254	30.2	12,522	2.99E-03	0.0988	6.88
S14	1937	274	34.8	13,742	3.17E-03	0.1225	9.58
S15	1519	205	13.9	9065	2.09E-03	0.0457	3.57
S16	1655	270	17.2	10,251	2.40E-03	0.0545	3.96
S17	1764	255	14.6	8105	1.74E-03	0.0818	8.91
S18	1838	216	21.8	11,792	2.69E-03	0.0797	5.81
S19	1941	178	22.6	11,186	2.70E-03	0.0901	7.19
S20	1957	26	21.4	11,187	2.57E-03	0.0839	6.78
S21	1761	252	21.3	10,769	2.40E-03	0.1118	10.90
S22	1835	281	11.2	7409	1.87E-03	0.0683	7.05
S23	1866	6	19.2	10,148	2.58E-03	0.0755	5.41
S24	1974	41	26.1	13,001	2.84E-03	0.0885	5.97
S25	1821	4	20.1	10,868	2.60E-03	0.0811	6.03
S26	1689	231	20.9	10,820	2.59E-03	0.0784	5.99
S27	1992	225	26.8	13,088	2.78E-03	0.1042	8.62
S28	1865	281	21.4	11,598	2.27E-03	0.1032	9.96
S29	1834	54	25.3	12,855	2.69E-03	0.0931	7.12
S30	1742	11	20.3	11,153	2.58E-03	0.0712	5.49
S31	2002	280	34.4	15,497	3.00E-03	0.1737	17.58
S32	2068	281	27.6	12,489	2.80E-03	0.1222	10.43

* Peak strain means the strain corresponds to the compressive strength.

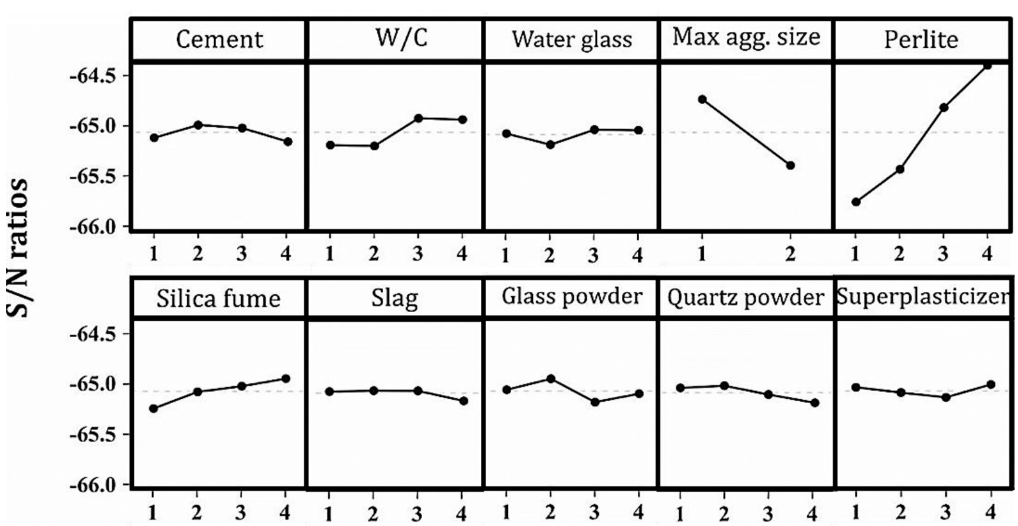

Fig. 8. Effect of variables on the density.

decrease slightly owing to the lower density of Silica fume compared to cement. However, Slag is not effective on the density. It can be attributed to the difference in the chemical structure of the Silica fume and Slag. Changes in the quantity of other variables (quartz and glass powders, and superplasticizer) have no significant influence on the PLWC density, as shown in Fig. 8).

3.3.2. Compressive strength

As shown in Fig. 9, PLWC's compressive strength is significantly affected by the amount of cement, so adding more cement enhances its strength. However, in level 2 (cement value of 450 kg/m^3) a decrease in compressive strength can be observed. This observation may be caused by the Perlite aggregates' separation as a result of the high slump value (see the mixtures S7, S8, and S22 information in Table 3 and Fig. 3). Increasing the water-to-cement ratio leads to a slight decrease in compressive strength. This shows that adding other components, such as water glass and pozzolans to the mixtures of PLWCs, can control the decreasing effect of water on the compressive strength. Moreover, water glass reduces the strength of cement paste [35], while increasing the consistency and adhesion of concrete and protecting it from separation

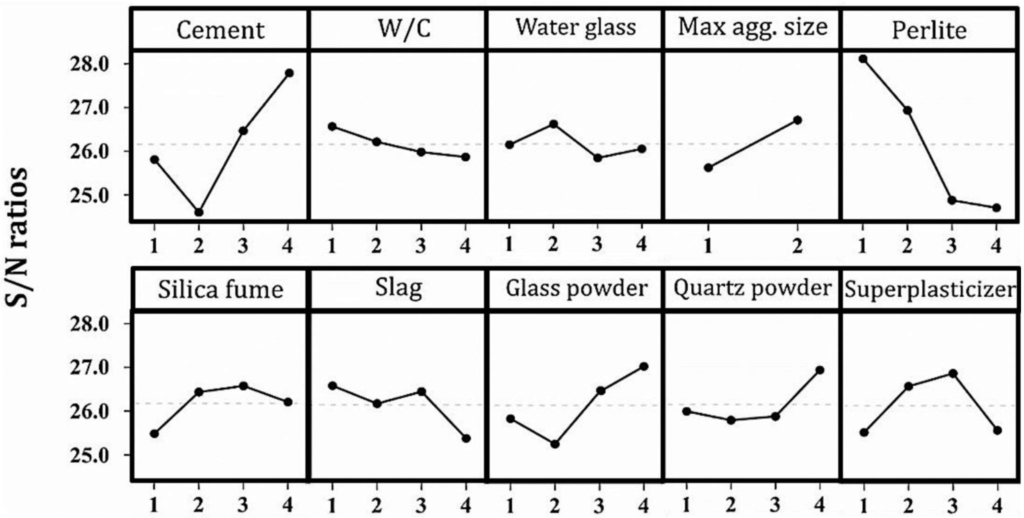

Fig. 9. Effect of variables on the compressive strength.

[35]. Therefore, its application is limited to the balance value, which can be 2.5 %wc, as shown in Fig. 9.

By increasing the maximum aggregate size, the value of compressive strength increases linearly. This is because of the greater load capacity of bigger aggregates than small ones. Since the Perlite aggregate has a lower strength than the normal aggregate, increasing the percentage of pearlite decreases the compressive strength.

The increase in Silica fume causes the compressive strength to rise somewhat and subsequently fall (see Fig. 9). The reason for the increase in strength can be the reduction of calcium hydroxide in the cement paste [12]. However, its excessive increase in the mix decreases the strength of the cement paste, due to a lack of calcium hydroxide to react with Silica fume [12]. Therefore, the limited value for using Silica fume is 12% volume percentage of cement. The compressive strength is approximately insensitive to the amount of Slag. However, adding Slag up to 10% volume percentage of cement enhances compressive strength [30], whereas up to 32% reduces compressive strength.

The results show that adding quartz and glass powders at level 4 significantly increases the compressive strength of PLWC. The main reason is related to the lower total porosity of PLWCs with a higher amount of filler. The use of superplasticizer up to level 3 (0.4 %wc) leads to an increase in compressive strength due to improved cement distribution and avoidance of particle buildup and lump formation. While by increasing the amount of superplasticizer up to 0.6 %wc, the compressive strength decreases considerably. The explanation might be a decrease in cement paste resistance.

3.3.3. *Energy absorption*

Increasing the quantity of cement reduces the energy dissipation capacity while increasing the energy dissipation rate marginally, as presented in Fig. 10 and Fig. 11. Although increasing the amount of cement leads the mortar strength to increase [5], the balance among the mortar strength, aggregates, and ITZ is disturbed. In this condition, dissipation energy strongly depends on the cracking in the ITZ zone and the crushing of Perlite aggregate. In contrast, increasing the w/c ratio enhances the total energy dissipation capacity while decreasing the energy dissipation rate. Small porosities in PLWCs may increase the deformation of PLWCs under compression, causing an increase in energy absorption. Similar behavior also can be found for the effect of water glass on the energy dissipation capacity and rate, owing to forming SiO_2 gel and inhibiting the hydration process [26].

By increasing the amount of Perlite, the energy dissipation capacity increases. However, it causes the energy dissipation rate to decrease up to level 3. As the process progresses to level 4, the trend of energy

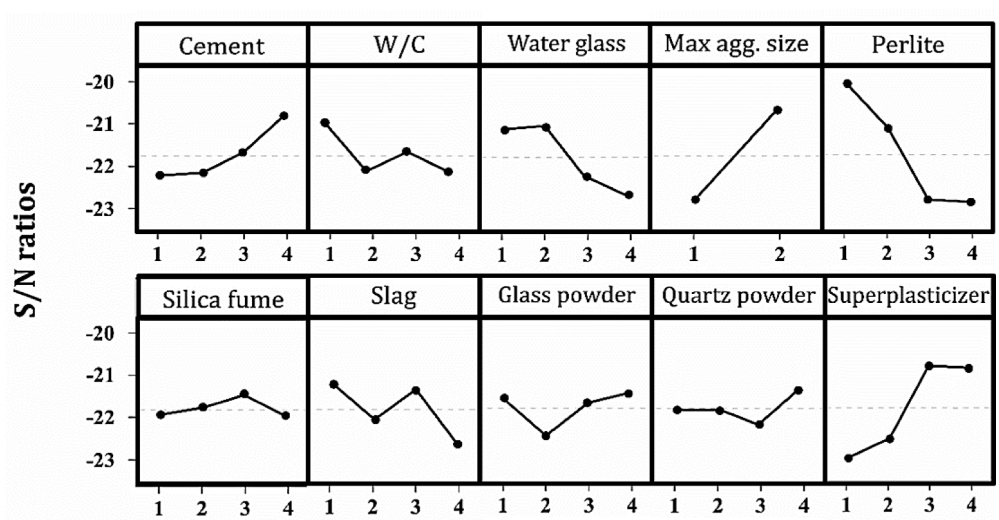

Fig. 10. Effect of variables on the energy dissipation capacity.

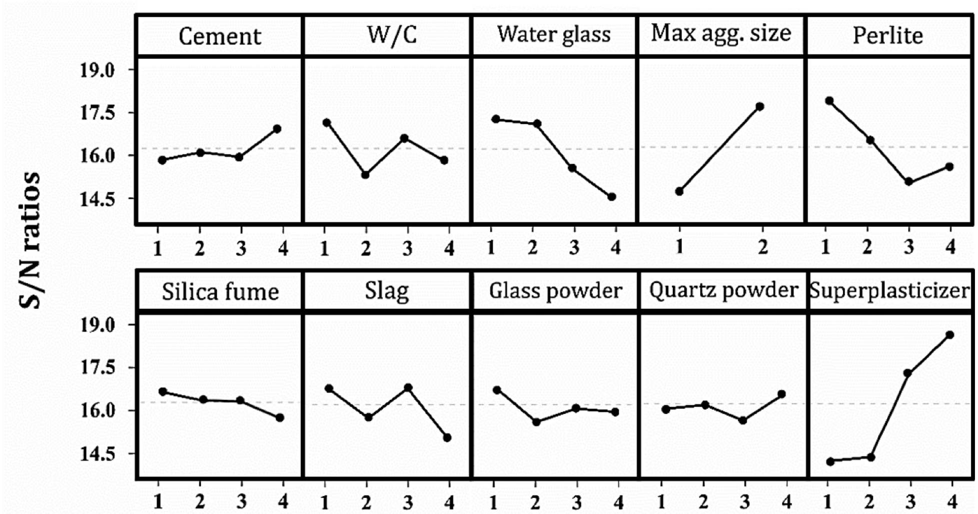

Fig. 11. Effect of variables on the energy dissipation rate.

dissipation rate reverses. To investigate the effect of Perlite on the energy dissipation capacity, its two opposite effects must be considered. On the one hand, the addition of Perlite as a porous aggregate reduces the compressive strength resulting in a low energy dissipation capacity of the specimen. On the other hand, its crushing dissipates the energy. As shown in Fig. 10, the amount of Perlite in level 3 can be considered an optimum condition. After this level, the negative effect of adding Perlite is significant and neutralizes its positive effect. In other words, the volume fraction of expanded Perlite plays a main role in the behavior of PLWC under compression by significantly changing the main parameters of compressive strength, peak strain, and total energy dissipation capacity. Increasing the amount of expanded Perlite to level 4 completely changes the behavior of PLWC (Fig. 12) due to its crushing under loading, which causes the axial strain to increase. Consequently, the energy dissipation capacity and rate of PLWC increase. Higher energy dissipation of PLWC improves its behavior in the failure condition and increases the failure time of the structure, which can be used as an important parameter in designing the structures, especially under impact loading [5].

Using a bigger size of normal aggregates leads to a decrease in the total energy dissipation capacity. Bigger normal aggregates cause the crushing of expanded Perlite aggregates during mixing and casting and decrease the positive effect of Perlite on the energy dissipation capacity of PLWC during compressive loading. Adding bigger normal aggregates increases the energy dissipation rate of PLWC, owing to the decreasing axial strain.

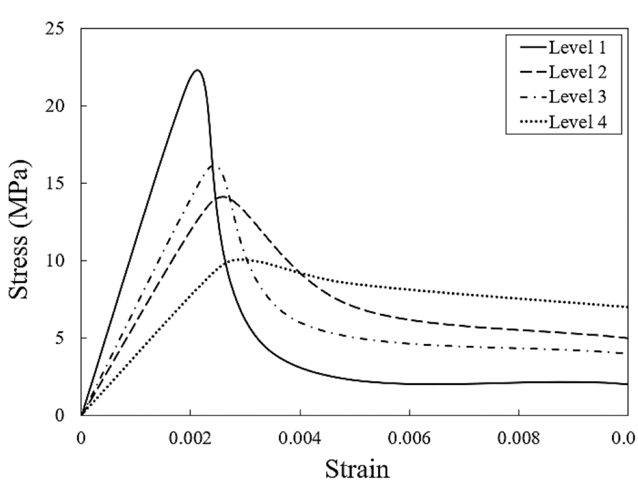

Fig. 12. Effect of expanded Perlite volume on the stress–strain behavior of PLWC.

Both the energy dissipation capacity and rate of PLWC decrease slightly with an increase in Silica fume and Slag. Adding the pozzolans (up to level 3) increases the compressive strength, while decreasing the ductility of the PLWCs and subsequently decreasing the energy dissipation capacity. Quartz and glass powder parameters do not affect the energy dissipation capacity of PLWCs significantly. Adding superplasticizer decreases the energy dissipation capacity, while it leads the energy dissipation rate to increase. This observation shows that in the mixtures included a higher superplasticizer, the segregation of Perlite aggregate is more likely. Non-uniformity of Perlite aggregate in PLWCs decreases the mechanical characteristics, such as energy dissipation capacity. While due to increases in axial strain, the energy dissipation rate increases with superplasticizer.

3.4. Modelling of compressive stress–strain curves of PLWC

In this section, the compressive strength (f_{co}) and its corresponding strain (ε_{co}), as well as the modulus of elasticity (E_c) of PLWCs, are predicted based on a model proposed by Lim and Ozbakkaloglu [49]. According to this model, the compressive parameters (f_{co}, ε_{co}, and E_c) are predicted based on the water-to-cement ratio (w/c), density (γ), and the Silica fume-to-cementitious matrix ratio (Sf/c). The Lim and Ozbakkaloglu model was developed based on the different lightweight aggregates (such as sintered diatomite, expanded clay, sintered fly ash, volcanic pumice, and tuff), so it should be modified for the expanded Perlite aggregates, as follows:

$$f_{co} = \left(\frac{21}{w/c} + 0.55\sqrt{Sf/c}\right)\left(\frac{\gamma}{2400}\right)^{3.14} \quad (1)$$

$$E_c = 2467\sqrt{f_{co}}\left(\frac{\gamma}{2400}\right)^{0.075} \quad (2)$$

$$\varepsilon_{co} = \frac{(f_{co})^{0.3k_d}}{1000}k_s\, k_a \quad (3a)$$

$$k_d = \left(\frac{2400}{\gamma}\right)^{0.1} \quad (3b)$$

$$k_s = \left(\frac{152}{D}\right)^{0.1} \quad (3c)$$

$$k_a = \left(\frac{2D}{H}\right)^{0.13} \tag{3d}$$

k_d, k_s, and k_a are the coefficients depending on the density, cylinder diameter (D), and its diameter to height ratio (D/H), respectively. Fig. 13 illustrates the comparison of the modified model as well as the Lim and Ozbakkaloglu model [49], with the experimental results. The modified model shows an accurate prediction. In addition, since the database for proposing these models included the structural and non-structural PLWCs, they can be utilized for both ranges of compressive strength. The results show that the effect of the geometry parameter D/H, the physical parameter γ, and different values of w/c and Sf/c for each type of lightweight concrete may be different. Therefore, the proposed models can be utilized for PLWCs and can be modified for other types of lightweight concrete. The Lim and Ozbakkaloglu model [49] slightly overestimates the values of f_{co} and E_c and underestimates the values of ε_{co}. It may be due to the effect of a different lightweight aggregate than that used in this study.

To evaluate the accuracy of the models, the mean absolute deviation (MAD) and mean absolute percentage error (MAPE) are used, based on Eqs. (4) and (5).

$$MAD = \left(\frac{1}{N}\right)\sum_{1}^{N}|pre_i - exp_i| \tag{4}$$

$$MAPE = \left(\frac{1}{N}\right)\sum_{1}^{N}\left|\frac{pre_i - exp_i}{exp_i}\right| \times 100 \tag{5}$$

where *pre* is the model predictions, exp is the experimental results, and N is the total number of specimens. The value of MAD and MAPE were calculated for each parameter. Table 5 shows the values of MAD and MAPE for the prediction results by different models. The results display that the values of MAPE and MAD for the Lim and Ozbakkaloglu model [49] are higher than the modified model presented in this study. It could be the result of using a different lightweight aggregate than that used in this study.

3.5. Modeling of energy dissipation capacity of PLWC

A unified expression is proposed to estimate the energy dissipate capacity (E_e) and rate ($\dot{\rho}_E$) of PLWC. As presented in section 3.3 and Fig. 10, the E_e increases with a reduction in the w/c ratio, Silica fume to cement ratio (Sf/c), and volume of Perlite aggregates (V_p). In addition, increasing density (γ) and amount of filler (F_a) cause the E_e to increase. Therefore, the effect of each parameter is statistically quantified through multivariable regression analysis, as presented in Eq. (6). The values of 0.2, 0.08, 0.55, 2400, and 2 are considered as the reference values of w/c ratio, Sf/c, γ, V_p, and F_a, respectively [12,27,49].

Table 5
MAPE and MAD values for prediction results by different models.

Parameter	Modified model		Lim and Ozbakkaloglu model [49]	
	MAPE	MAD	MAPE	MAD
Compressive strength (f_{co})	12.11	2.29	35.49	6.41
Modulus of elasticity (E_c)	4.09	439.39	19.00	2131.37
Peak strain (ε_{co})	5.64	0.00013	13.57	0.00036

$$E_e = \left(\frac{0.2}{w/c}\right)^{5.39}\cdot\left(\frac{0.08}{0.01+Sf/c}\right)^{0.06}\cdot\left(\frac{0.55}{V_p}\right)^{0.42}\cdot\left(\frac{\gamma}{2400}\right)^{1.72}\cdot(F_a+2)^{0.02} \tag{6}$$

The analysis of the proposed model for the energy dissipation capacity of PLWC suggests that it performs reasonably well in predicting experimental outcomes. Evaluation metrics such as Mean/Median of prediction, Standard Deviation of prediction, Range of prediction, and Coefficient of Determination (R^2) can be used to assess the proposed models in relation to experimental results [50]. The mean and median of the predictions are both 0.06 and 0.07, respectively, falling within an acceptable range and indicating that the model provides reliable outcome estimates. The model's standard deviation of predictions is relatively low, at 3.5%, which suggests that it has good precision in its estimates. Additionally, the model can capture a wide range of possible outcomes, with a reasonable range of predictions at 0.13. Finally, the coefficient of determination ($R^2 = 0.91$) is relatively high, suggesting that the model can explain a significant proportion of the variability in the data. In conclusion, these results indicate that the proposed model is a promising tool for predicting similar experiments' outcomes in the future.

Regarding the energy dissipation rate ($\dot{\rho}_E$), three main parameters of compressive strength (f_{co}), density (γ), and volume of Perlite aggregate (V_p) are considered as independent variables to propose a new model. The results display that the $\dot{\rho}_E$ of PLWCs slightly increases with an increase in f_{co} (Table 4). Moreover, although adding the Perlite decreases the density of PLWCs the Perlite aggregates cause the PLWCs to dissipate energy at a higher rate (Table 4). Eq. (7) presents a developed model to predict the energy dissipation rate of PLWCs.

$$\dot{\rho}_E = 0.22 \times (f_{co})^{0.67}\cdot\left(\frac{V_p}{0.55}\right)^{0.41}\cdot\left(\frac{\gamma}{2400}\right)^{2.06} \tag{7}$$

The proposed model performs well in predicting the experimental energy dissipation rate, as indicated by the mean (5.95) and median (6.23) falling within an acceptable range, low standard deviation of predictions (2.6%), reasonable range of predictions (12.23), and high coefficient of determination ($R^2 = 0.91$). Therefore, the model is a promising tool for future predictions, but further testing and refinement may be necessary.

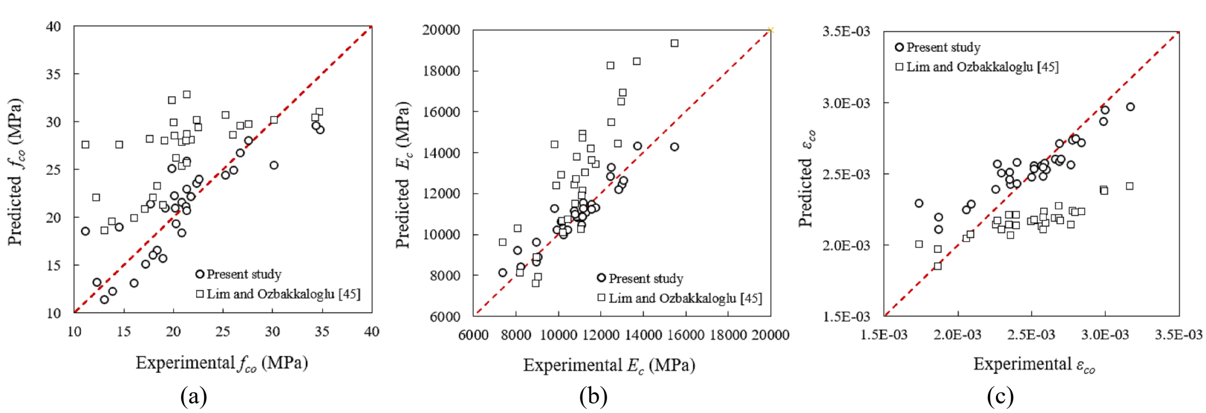

Fig. 13. Comparison of the experimental and predicted results by the present study and Lim and Ozbakkaloglu [49]: (a) Compressive strength; (b) Modulus of elasticity; (c) Strain corresponds to the compressive strength.

Fig. 14 shows that the predictions of the proposed expression for both E_e and $\dot{\rho}_E$ are in good agreement with the experimental results obtained in the present study and other research [5,51]. As can be seen in Fig. 14, the maximum error in predictions of both energy dissipation capacity and energy dissipation rate is limited to 25% (dashed lines in the figures). The obtained error may be related to the chemical and physical composition of the used components in PLWCs mixtures such as Silica fume and expanded Perlite aggregates which can affect the compressive behavior of the PLWCs. More research is essential to perform in the microstructural level to investigate the effect of the chemical and physical composition of the components on the compressive behavior of PLWCs.

3.6. Selecting the best mixture

A quality function can be defined by considering the physical and mechanical properties to achieve the highest quality for PLWC, based on [5]. For this purpose, four concepts are considered in determining the quality function: (a) the low bulk density (γ, kg/m^3), (b) the high compressive strength (f_{co}, MPa), (c) the high energy dissipation capacity (E_e, J), and (d) the high energy dissipation rate ($\dot{\rho}_E$, J). According to the four mentioned concepts, the quality index (QI) is proposed and defined as follows:

$$QI = \left[\frac{f_{co} - \alpha(f_{co} - 17)}{17}\right] \cdot \left(\frac{1850}{\gamma}\right) \cdot (100 \times E_e) \cdot \left(\dot{\rho}_E\right) \quad (8)$$

For $f_{co} < 17$ MPa (as nonstructural concrete [52]), f_{co} directly affects the QI, while for higher values of f_{co} (as structural concrete [52]), its effect is decreased by a variable coefficient (α). The α is defined to address the main aims of using PLWC (low weight and capacity to dissipate energy) which is a linear function of f_{co} and increases with it, as presented in Fig. 15.

In terms of density, the *QI* has an inverse relationship with the density of concrete, the lower density, the higher quality index. Regarding energy dissipation capacity, since the values of the E_e and $\dot{\rho}_E$ have high differences, the increasing coefficient of 100 is used for E_e value to make them comparable. This coefficient leads to considering the effect of all parameters at the same level. Due to the necessity of a bulk density lower than 1850 kg/m^3 (according to ACI 318 [52]), mixtures with higher bulk density were eliminated, as shown in Fig. 16.

Table 6 reports the quality index of accepted mixtures with compressive strength higher than 17 MPa and density less than 1850 Kg/m^3. The results show that sample S21 has the best performance by QI equal to 135.99. This mixture includes 100% Perlite replacement with normal aggregates, 36 %wc of pozzolans, 30 %wc of fillers, 2.5 % wc of water glass, and 0.4 %wc of the superplasticizer. The values of the bulk density and compressive strength for the mixture of S21 are 1761 kg/m^3 and 21.3 MPa, respectively. The main reason for the higher

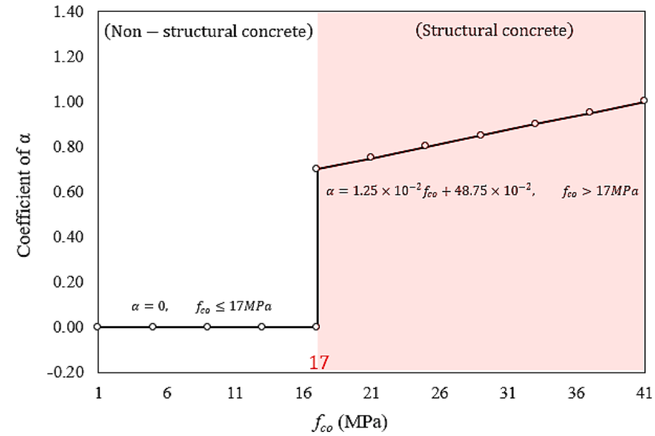

Fig. 15. Alpha (α) coefficient.

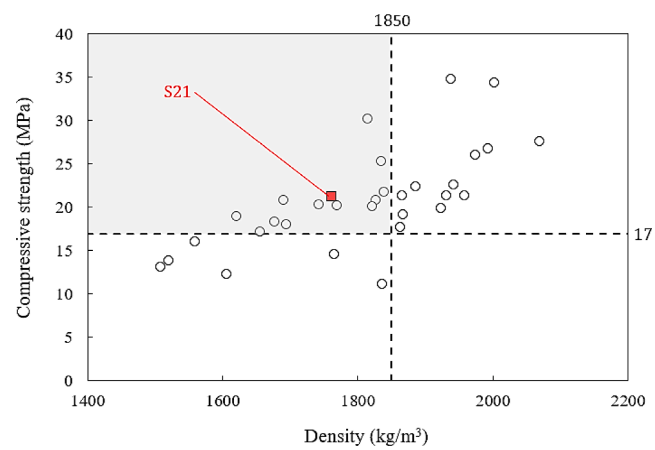

Fig. 16. Criteria for structural lightweight concrete.

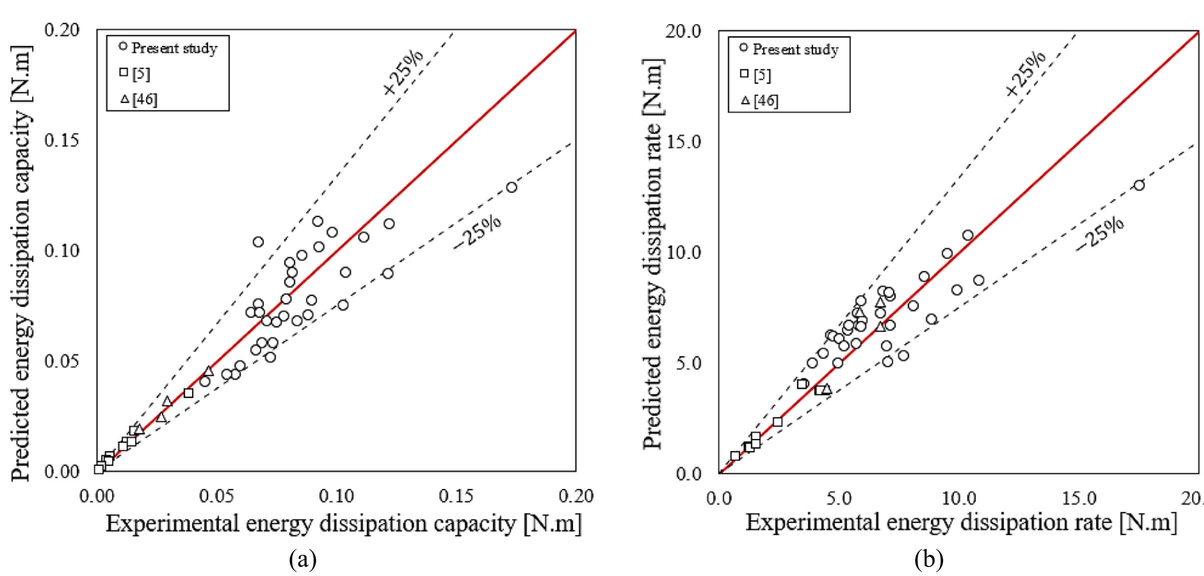

Fig. 14. Comparison of the experimental and predicted results: (a) Energy dissipation capacity; (b) Energy dissipation rate.

Table 6
Quality index of accepted mixtures *.

Specimen ID	Quality Index	Specimen ID	Quality Index
S2	32.53	S18	49.77
S3	45.29	S21	135.99
S9	67.77	S25	52.05
S11	41.33	S26	54.40
S12	29.43	S29	73.27
S13	76.59	S30	43.60
S16	24.21		

* Bulk density < 1850 kg/m^3 and Compressive strength > 17 MPa

quality index of this mixture (S21) rather than other acceptable mixtures is its higher energy dissipation capacity and rate ($E_e = 0.1118\ J$ and $\dot{\rho}_E = 10.90\ J$).

4. Conclusion

This paper investigated the material properties of Perlite lightweight concrete (PLWC) by considering the effect of water, cement, pozzolan (Silica fume and Slag), water glass, superplasticizer, maximum aggregate size, and volume of Perlite aggregates. Taguchi method (included ten variables in 4 levels) was used to determine the effect of each component and to select the optimal mixtures of PLWC by considering the four main parameters of density, compressive strength, energy dissipation capacity, and energy dissipation rate. Based on the findings of this study, the following conclusions are drawn:

(1) Aggregate size and Perlite had a significant effect on the PLWC density. By increasing the maximum aggregate size, ITZ zone surfaces decreased, resulting in an increase in density. Furthermore, adding Perlite as a porous lightweight aggregate appreciably decreased the density.

(2) The amount of cement and Perlite were the most effective parameters on the compressive strength of PLWC. Increasing the amount of cement led to an increase in strength. As expected, since the Perlite aggregate had a lower strength than the normal aggregate, increasing the percentage of pearlite decreased the compressive strength.

(3) However, all components are effective on both energy dissipation capacity and energy dissipation rate, the effect of adding expanded Perlite, maximum aggregate size, and water glass were more significant than others. Adding aggregate with a higher maximum aggregate size increased the energy dissipation capacity and energy dissipation rate of PLWC. The results showed that adding water glass increased the adhesion of the matrix and aggregate although significantly decreased both energy dissipation capacity and energy dissipation rate. Increasing the amount of Perlite up to 85% decreased the energy dissipation capacity and energy dissipation rate. While adding more amount of Perlite (100%) indicated an increase in these parameters. The addition of Perlite as a porous aggregate reduced the resistance of the specimen, while its crushing dissipated energy. Although by increasing the amount of expanded Perlite, the compressive strength decreased, the post-peak behavior of PLWC was completely changed and the rate of energy dissipation rose.

(4) New models for compressive strength, modulus of elasticity, peak strain, energy dissipation capacity and rate were proposed to express the compressive behavior of PLWCs. The evaluation of the new models showed that the proposed models could predict the experimental results satisfactorily. The model was applicable for Perlite lightweight concretes with compressive strengths up to 40 MPa. The important features of the proposed models included: (i) applicability to concretes with various densities and compressive strengths, (ii) accurate prediction of the compressive strength, modulus of elasticity, and peak strain of PLWCs, and (iii) consideration of the change in energy dissipation capacity and rate with the different PLWCs.

The study demonstrated that expanding Perlite as lightweight aggregates in concrete could be one of the most practical methods for designing lightweight structural concrete. There are, however, some parameters that need to be examined in future studies, including the effects of expanded Perlite surface treatment and porosity on lightweight concrete behavior under compressive load. It is also necessary to address in future studies the behavior of PLWC specimens under different loading (e.g., cyclic and dynamic) and loading rates.

CRediT authorship contribution statement

Mohammad Bakhshi: Methodology, Software, Validation, Visualization, Writing – original draft. **Ali Dalalbashi:** Conceptualization, Supervision, Writing – review & editing. **Hassan Soheili:** Conceptualization, Visualization, Investigation, Writing – review & editing.

Declaration of Competing Interest

The authors declare that they have no known competing financial interests or personal relationships that could have appeared to influence the work reported in this paper.

Data availability

Data will be made available on request.

Acknowledgment

The authors would like to acknowledge the assistance given by the technical staff of the structural laboratory of Tarbiat Modares University. Moreover, this research did not receive any grant.

References

[1] O. Sengul, S. Azizi, F. Karaosmanoglu, M.A. Tasdemir, Effect of expanded perlite on the mechanical properties and thermal conductivity of lightweight concrete, Energy Build. 43 (2-3) (2011) 671–676.
[2] M.M. Atyia, M.G. Mahdy, M. Abd Elrahman, Production and properties of lightweight concrete incorporating recycled waste crushed clay bricks, Constr. Build. Mater. 304 (2021), 124655.
[3] S. Rattanachan, C. Lorprayoon, Korat clays as raw materials for lightweight aggregates, Sci. Asia 31 (2005) 277–281.
[4] M. Bakhshi, S. Shahbeyk, Experimental and microstructural study of the compressive strength of concrete samples containing low volumes of expanded polystyrene beads, Struct. Concr. 20 (4) (2019) 1379–1390.
[5] M. Bakhshi, H. Soheili, A. Dalalbashi, Optimization of a structural lightweight fiber-reinforced concrete for best performance under impact loading, Cem. Concr. Compos. 136 (2023) 104875.
[6] X.G. Zhang, X.M. Kuang, J.H. Yang, S.R. Wang, Experimental study on mechanical properties of lightweight concrete with shale aggregate replaced partially by nature sand, Electron. J. Struct. Eng. 17 (2017) 85–94.
[7] K.M. Anwar Hossain, Properties of volcanic pumice based cement and lightweight concrete, Cem. Concr. Res. 34 (2) (2004) 283–291.
[8] D. Sari, A.G. Pasamehmetoglu, The effects of gradation and admixture on the pumice lightweight aggregate concrete, Cem. Concr. Res. 35 (5) (2005) 936–942.
[9] D. Bouvard, J.M. Chaix, R. Dendievel, A. Fazekas, J.M. Létang, G. Peix, D. Quenard, Characterization and simulation of microstructure and properties of EPS lightweight concrete, Cem. Concr. Res. 37 (12) (2007) 1666–1673.
[10] B. Berge, Ecology of building materials, Routledge, 2007.
[11] İ.B. Topçu, B. Işıkdağ, Effect of expanded perlite aggregate on the properties of lightweight concrete, J. Mater. Process. Technol. 204 (1-3) (2008) 34–38.
[12] R. Demirboga, R. Gül, The effects of expanded perlite aggregate, silica fume and fly ash on the thermal conductivity of lightweight concrete, Cem. Concr. Res. 33 (2003) 723–727, https://doi.org/10.1016/S0008-8846(02)01032-3.
[13] R. Demirboğa, İ. Örüng, R. Gül, Effects of expanded perlite aggregate and mineral admixtures on the compressive strength of low-density concretes, Cem. Concr. Res. 31 (11) (2001) 1627–1632.
[14] M. Jedidi, O. Benjeddou, C. Soussi, Effect of expanded perlite aggregate dosage on properties of lightweight concrete, Jordan J. Civ. Eng. 9 (3) (2015) 378–391.
[15] M. Ibrahim, A. Ahmad, M.S. Barry, L.M. Alhems, A.C. Mohamed Suhoothi, Durability of structural lightweight concrete containing expanded perlite aggregate, Int. J. Concr. Struct. Mater. 14 (2020) 1–15.

[16] M. Singh, M. Garg, Perlite-based building materials—a review of current applications, Constr. Build. Mater. 5 (2) (1991) 75–81.
[17] N. Burriesci, C. Arcoraci, PierLuigi Antonucci, G. Polizzotti, Physico-chemical characterization of perlite of various origins, Mater. Lett. 3 (3) (1985) 103–110.
[18] J. Esfandiari, P. Loghmani, Effect of perlite powder and silica fume on the compressive strength and microstructural characterization of self-compacting concrete with lime-cement binder, Measurement. 147 (2019), 106846.
[19] H.E. M. Ghannadi, Y. Zandi, Effect of Microsilis, Super Plasticizer and Air Entrain in Lightweight Perlite Concrete Prepared by Microsilis and Super Plasticizer, in: Int. Conf. Concr. Technol. Tabriz, 2009.
[20] V. Revilla-Cuesta, M. Skaf, A. Santamaría, V. Ortega-López, J.M. Manso, Assessment of longitudinal and transversal plastic behavior of recycled aggregate self-compacting concrete: A two-way study, Constr. Build. Mater. 292 (2021) 123426.
[21] V. Revilla-Cuesta, V. Ortega-López, M. Skaf, J.M. Manso, Deformational behavior of self-compacting concrete containing recycled aggregate, slag cement and green powders under compression and bending: Description and prediction adjustment, J. Build. Eng. 54 (2022), 104611.
[22] M. Bakhshi, I.B. Valente, H. Ramezansefat, J.A.O. Barros, E.N.B. Pereira, N.R. M. Peixinho, Experimental and analytical study of the high-strain-rate compressive behavior of SFRC, Mech. Adv. Mater. Struct. 1–24 (2023).
[23] V. Ortega-Lopez, A. Garcia-Llona, V. Revilla-Cuesta, A. Santamaría, J.T. San-Jose, Fiber-reinforcement and its effects on the mechanical properties of high-workability concretes manufactured with slag as aggregate and binder, J. Build. Eng. 43 (2021), 102548.
[24] A. C150/C150M-20, Standard specification for Portland cement, Tech. Report, ASTM Int. West Conshohocken, PA. (2020).
[25] ASTM C187 -16, American Society for Testing and Materials, Standard Test Method for Amount of Water Required for Normal Consistency of Hydraulic Cement Paste, ASTM Int. Pennsylvania. (2016).
[26] J. Larosa-Thomson, P. Gill, B.E. Scheetz, M.R. Silsbee, Sodium silicate applications for cement and concrete, Proc. 10th Int Congr. Chem. Cem. Gothenbg. 3 (1997) 3.
[27] H. Moosberg-Bustnes, B. Lagerblad, E. Forssberg, The function of fillers in concrete, Mater. Struct. 37 (2) (2004) 74–81.
[28] P. Mondal, S.P. Shah, L.D. Marks, J.J. Gaitero, Comparative study of the effects of microsilica and nanosilica in concrete, Transp. Res. Rec. 2141 (1) (2010) 6–9.
[29] V. Ajay, C. Rajeev, R.K. Yadav, Effect of micro silica on the strength of concrete with ordinary Portland cement, Res. J. Eng. Sci. 2278 (2012) 9472.
[30] H.-S. Lee, X.-Y. Wang, L.-N. Zhang, K.-T. Koh, Analysis of the optimum usage of slag for the compressive strength of concrete, Materials (Basel) 8 (2015) 1213–1229.
[31] S.K. Karna, R. Sahai, An overview on Taguchi method, Int. J. Eng. Math. Sci. 1 (2012) 1–7.
[32] M. Arifuzzaman, H.S. Kim, Novel mechanical behaviour of perlite/sodium silicate composites, Constr. Build. Mater. 93 (2015) 230–240.
[33] A. El Mir, S.G. Nehme, Utilization of industrial waste perlite powder in self-compacting concrete, J. Clean. Prod. 156 (2017) 507–517.
[34] L.-H. Yu, H. Ou, L.-L. Lee, Investigation on pozzolanic effect of perlite powder in concrete, Cem. Concr. Res. 33 (1) (2003) 73–76.
[35] M.D. Arifuzzaman, H.S. Kim, Development of new perlite/sodium silicate composites, in: Int. Conf. Mech. Ind. Energy Eng. (ICMIEE), Khulna Univ. Eng. Technol. Khulna, Bangladesh, 2014: p. 27.
[36] R.K. Roy, A primer on the Taguchi method, Society of Manufacturing Engineers, 2010.
[37] AASHTO T85, Standard Method of Test for Specific Gravity and Absorption of Coarse Aggregate, 2022.
[38] C.S. Poon, Z.H. Shui, L. Lam, Effect of microstructure of ITZ on compressive strength of concrete prepared with recycled aggregates, Constr. Build. Mater. 18 (6) (2004) 461–468.
[39] C. ASTM, Standard practice for capping cylindrical concrete specimens, C617M-15. (2015).
[40] A. ASTM, ASTM C143. Standard test method for slump of hydraulic cement concrete, 1988.
[41] C. Astm, 138., Standard Test Method for Density (Unit Weight), Yield, and Air Content (Gravimetric) of Concrete, PA ASTM Int, West Conshohocken, 2014, p. 2015.
[42] A. ASTM, ASTM C39/C39M-18 standard test method for compressive strength of cylindrical concrete specimens, ASTM Int. West Conshohocken, PA. ASTM, AI (2018).“ ASTM C. 192 (2018).
[43] ASTM C469/C469M, Standard Test Method for Static Modulus of Elasticity and Poisson’s Ratio of Concrete in Compression, 2022.
[44] V. Vosoughi, S.M.M. Crin, S. Eisapour, Evaluation of perlite powder Performance in concrete to replace part of the cement, Fen Bilim. Derg. 36 (2015).
[45] M. Rezaie, N. Sadighi, Prediction of slump and density of lightweight concretes using ANFIS and linear regression, Int. J. Civ. Eng. Technol. 8 (2017) 1635–1648.
[46] A. Kan, R. Demirboğa, A novel material for lightweight concrete production, Cem. Concr. Compos. 31 (7) (2009) 489–495.
[47] R. Şahin, R. Demirboğa, H. Uysal, R. Gül, The effects of different cement dosages, slumps and pumice aggregate ratios on the compressive strength and densities of concrete, Cem. Concr. Res. 33 (8) (2003) 1245–1249.
[48] T. Akçaoğlu, M. Tokyay, T. Çelik, Effect of coarse aggregate size and matrix quality on ITZ and failure behavior of concrete under uniaxial compression, Cem. Concr. Compos. 26 (6) (2004) 633–638.
[49] J.C. Lim, T. Ozbakkaloglu, Stress–strain model for normal-and light-weight concretes under uniaxial and triaxial compression, Constr. Build. Mater. 71 (2014) 492–509.
[50] J. Feng, G. Yin, H. Tuo, Z. Niu, Parameter optimization and regression analysis for multi-index of hybrid fiber-reinforced recycled coarse aggregate concrete using orthogonal experimental design, Constr. Build. Mater. 267 (2021), 121013.
[51] D.S. Law Yim Wan, F. Aslani, G. Ma,, Lightweight self-compacting concrete incorporating perlite, scoria, and polystyrene aggregates, J. Mater. Civ. Eng. 30 (2018) 4018178.
[52] A.C.I.A.C.I. Committee, Building Code Requirements for Structural Concrete ACI 318-19 and Commentary 318R–19, Am. Concr. Inst. ACI Comm. Farmingt. Hills, MI, USA. (2019).